Parametric and Convergence Studies of the Smoothed Particle Galerkin (SPG) Method in Semi-brittle and Ductile Material Failure Analyses

Youcai Wu, C.T. Wu, Wei Hu

Livermore Software Technology Corporation (LSTC)
7374 Las Positas Road, Livermore, CA 94551, U.S.A.

Abstract

This work presents the state-of-the-art status of the Smoothed Particle Galerkin (SPG) method [1, 2] in LS-DYNA®. The SPG method is a new generation meshfree method developed for modeling the semi-brittle and ductile material failure [3-5]. Different from the conventional finite element method (FEM) where the element erosion technique is utilized to mimic the material separation, the SPG method introduces a bond-based material failure criterion to reproduce the strong discontinuity in displacement field without sacrificing the conservation properties of the system equations. The mathematical and numerical analyses have suggested that the SPG scheme is stable and convergent in modeling material failure processes.

Currently, one of the major applications of the SPG method is the simulation of destructive manufacturing processes such as riveting, screwing, drilling and machining. The SPG method also can be applied to model the material failure in high velocity impact penetration problems. In this work, we will present several analyses where the SPG method is employed to model the semi-brittle and ductile material failure phenomena in industrial applications. To illustrate the effectiveness of the SPG method in those applications, some parametric and convergence studies including the effects of failure criterion, nodal support size and domain discretization will be discussed. Several modeling issues including the material constitutive law, related LS-DYNA keywords and types of SPG formulations will also be elaborated.

Keywords: smoothed particle Galerkin (SPG), convergence, failure

1. Introduction

In crashworthiness tests in automotive industry, the failure in base and connection materials governs the crash modes, which in turn determines the protection level to the occupants. Therefore, the failure behavior must be captured as accurate as possible. It is time and cost demanding to predict failure using experimental characterization and calibration. The demand could be significantly reduced if an effective numerical approach that can predict failure reliably can be applied.

As a matured numerical method, the finite element method (FEM) has been successfully applied in numerous industrial simulations since its development in the 1940s. However, it is well known that traditional FEM has difficulty in failure analysis due to its assumption of continuous displacement field. Element erosion technique is usually applied to introduce displacement discontinuity in FEM for failure analysis, which leads to loss of mass, momentum, and energy. Furthermore, the erosion criterion is element size and problem dependent. As a result, the force response is usually underestimated and the failure pattern cannot be captured physically. These issues have largely limited the application of traditional FEM in material failure analysis.

Meshfree methods, on the other hand, known to be able to handle large material distortion, moving boundary and free surface, and moving discontinuity, boomed in the 1990s, has showed some potential in the prediction of material failure. Among the many meshfree methods, the smoothed particle Galerkin (SPG) method [1, 2] was developed particularly for modeling material failure in ductile and semi-brittle materials. The

theory and some applications of the SPG method are well documented in the literature [1-5]. The SPG method is a genuine particle method which does not use any mesh, not even for the spatial domain integration. The notorious issues encountered in application of meshfree methods in material failure analysis such as low energy modes, tension instability, strain localization, and excessive straining are addressed in the SPG formulation. The low energy modes are suppressed by a penalty based stabilization term derived from displacement smoothing without any parameter tuning. The tension instability is mitigated by proposing an anisotropic updated Lagrangian kernel. The strain localization induced by material instability is regularized by a morphing algorithm [6]. The excessive straining is overcome by introducing strong discontinuity on the displacement field, which uses a phenomenological bond based failure mechanism to fail and separate material. The failure criterion can be easily defined in phenomenological material constitutive laws. The SPG formulation has been uniquely implemented into LS-DYNA®. To show the effectiveness of the SPG method in material failure analysis, this paper presents the convergence and parametric studies of the SPG method in modeling failure of ductile and semi-brittle materials.

2. LS-DYNA keywords for SPG analysis

Figure 1 illustrates the up-to-date (March 2018) setup for an SPG analysis, which has minimized the requirements for user input from its original implementation.

The SPG analysis starts with an exactly same discretization as for a three-dimensional FEM analysis with solid elements. All geometrical shapes of solid elements, e.g., tetrahedron, pentahedron, hexahedron, heptahedron, and octahedron are accepted by the SPG formulation. The only difference is that the "SECID" parameter on the "*PART" card needs to be flagged to "*SECTION_SOLID_SPG" instead of "*SECTION_SOLID". It should be emphasized that "ELFORM" on the "*SECTION_SOLID_SPG" card must be set to 47 for an SPG analysis, although "SPG" has been include in the keyword title. The exact same "*ELEMENT_SOLID" is used for the input of element connections, which are only used in the calculation of initial mass and volume of each node.

Most of the parameters on the "*SECTION_SOLID_SPG" card can take the default values, which are defined in Table 1. While all the other parameters can leave blank on the input cards, the user must select an appropriate kernel function ("KERNEL") according to the deformation characteristics and the failure criteria according to the properties of the materials. Reasonably physical parameters (failure criteria) are expected for the numerical response to be physical.

```
*PART
SPG
$#       PID       SECID       MID      EOSID       HGID       GRAV     ADPOPT       TMID
           1           1        3615       3615          0          0          0          0
*SECTION_SOLID_SPG
$#     SECID      ELFORM        AET
           1          47          0
$#        DX          DY         DZ    ISPLINE     KERNEL     LSCALE     SMSTEP     SWTIME
                                                        1
$#      IDAM          FS    STRETCH        ITB                   ISC
                    0.45       1.25
```

Figure 1. Setup for SPG analysis.

Table 1 Parameters of SPG method

Parameter	Meaning and default
ELFORM	Must be 47

DX, DY, DZ	Normalized support size
	Default: 1.5 if KERNEL=2
	          1.6 if KERNEL=0
	          1.8 if KERNEL=1

ISPLINE	Kernel function type Default: 0 – cubic B-Spline function
KERNEL	Kernel type =0: update Lagrangian, tension dominant problems =1: Eulerian kernel, large and extreme deformation, global response =2: pseudo-Lagrangian kernel, extreme deformation, local response

SMSTEP	Interval of time steps for kernel update
	Default: 15 if KERNEL=0
	          5 if KERNEL=1
	          30 if KERNEL=2

IDAM	Damage indictor =0: continuum damage mechanics (obsolete) =1: effective plastic strain (default) =2: 1st principal stress
FS	Effective plastic strain at failure for IDAM=1, otherwise, not used
STRETCH	Relative stretch ratio for bond failure, not used if IDAM≠0
ITB	Stabilization indicator Default: 1 if KERNEL=0 or 1 2 if KERNEL=2
ISC	Indicator for self-contact between failed particles in impact penetration analysis, user should input Young's modulus of the material to activate it

3. SPG bond-based failure mechanism

A bond-based failure mechanism is implemented in the SPG framework so that displacement discontinuity (i.e., material failure and separation) can be captured and furthermore, the spurious damage growth in extremely large deformation events can be prevented. It is named "bond-based" because it treats the interaction between two neighboring nodes as a chemical bond, which could be broken when certain criteria are satisfied. In specific, two neighboring particles are considered disconnected during the meshfree neighbor particle searching whenever their averaged effective plastic strain and relative stretch ratio reach their respective critical values. In other words, for a pair of nodes K and J, the SPG shape function can be defined as:

$$\Phi_K(\mathbf{x}_J) = \begin{cases} 0 & \text{if } \bar{\varepsilon}^p_{KJ} > \bar{\varepsilon}^p_{crit} \text{ and } e_{KJ} > e_{crit} \\ \sum_{I=1}^{NP} \Psi_I(\mathbf{x}_J)\Psi_K(\mathbf{x}_I) & \text{Otherwise} \end{cases} \qquad (1)$$

where $\bar{\varepsilon}_{KJ}^{p} = \left[\bar{\varepsilon}^{p}(\mathbf{x}_K) + \bar{\varepsilon}^{p}(\mathbf{x}_J) \right]/2$ is the averaged effective plastic strain at nodes K and J and $\bar{\varepsilon}_{crit}^{p}$ is its critical value; $e_{KJ} = \|\mathbf{x}_K - \mathbf{x}_J\| / \|\mathbf{X}_K - \mathbf{X}_J\|$ is the relative stretch ratio between nodes K and J, where $\mathbf{x}$ and $\mathbf{X}$ are the current and reference coordinates.

The bond failure mechanism is illustrated in Figure 2. The support of node 2 covers nodes 1, 3, 8, 9, 10 besides itself. Therefore, there are 5 bonds, i.e., 2-1, 2-3, 2-8, 2-9, and 2-10 connected to node 2. Similarly, there are 7 bonds, i.e., bonds 1-2, 1-4, 1-5, 1-6, 1-7, 1-8, and 1-10 connected to node 1. If $\bar{\varepsilon}_{12}^{p} = \left[\bar{\varepsilon}^{p}(\mathbf{x}_1) + \bar{\varepsilon}^{p}(\mathbf{x}_2) \right]/2 > \bar{\varepsilon}_{crit}^{p}$ and $e_{12} > e_{crit}$ are satisfied simultaneously, then bond 1-2 (or 2-1) is broken. Therefore, $\Phi_2(\mathbf{x}_1) = 0$ and $\Phi_1(\mathbf{x}_2) = 0$. However, $\Phi_2(\mathbf{x}_k) \neq 0$ $k = 3, 8, 9, 10$ and $\Phi_1(\mathbf{x}_k) \neq 0$ $k = 4, 5, 6, 7, 8, 10$, which means all other bonds are still connecting. As a consequence, the state variables (i.e., stress and strain) at nodes 1 and 2 will still evolve regularly according to the deformation and material law. The only change is that node 2 is not involved in the calculation of node 1, and vice versa, although spatially their supports might still cover each other.

Therefore, unlike the finite element failure mechanism, where the element is eroded (loss of mass) according to an ad-hoc criterion and the element stress is set to zero (loss of momentum) when failure occurs, which often leads to underestimate of reaction forces and nonphysical failure pattern, the SPG bond failure mechanism preserves the mass and momentum, which provides the potential to predict more accurate force and more physical failure modes.

It should also be pointed out that since the effective plastic strain at each particle is monotonically increasing during the course of deformation, the kinematic disconnection (i.e., bond failure) between two particles in a pair is considered as a permanent and irreversible process. This is a substantial characteristic of the SPG method in material failure analysis since the nonphysical material self-healing issue is completely exempted from the modeling of the failure process using Eulerian approach.
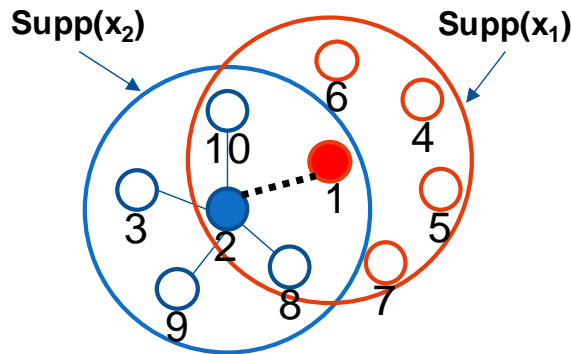

Figure 2. Illustration of SPG bond failure mechanism.

4. SPG for ductile failure analysis

In this section, the performance of the SPG method in ductile failure analysis is evaluated through a three-dimensional metal machining simulation. The experimental test was conducted at ITRI (industrial technology

research institute, Taiwan) [3] and the reaction forces are recorded for comparison purpose. Convergence and sensitivity studies of major SPG parameters are also performed.

4.1. Geometry and discretization

Figure 3 (a) shows the dimensions of the test article. The workpiece is clamped at the bottom. The cutter, which has a diameter of 10 mm, is made of hardened mild steel and is modeled as rigid (FEM). The cutter rotates at 8000 rpm while translating at 3000mm/min in the x-direction (Figure 3 (b)). The cutting depth and cutting thickness are 10 mm and 1 mm respectively. The material of the workpiece is 6061-T6 aluminum alloy, which is modeled by the Johnson-Cook material model. No lubricant is used in the test. Therefore clean and dry surfaces are assumed in the simulation. The SPG bond failure mechanism is employed to model the material failure, separation, and cutting debris in the extremely large deformation process of metal machining such that excessive straining and spurious damage growth issues are eliminated from the numerical simulation.

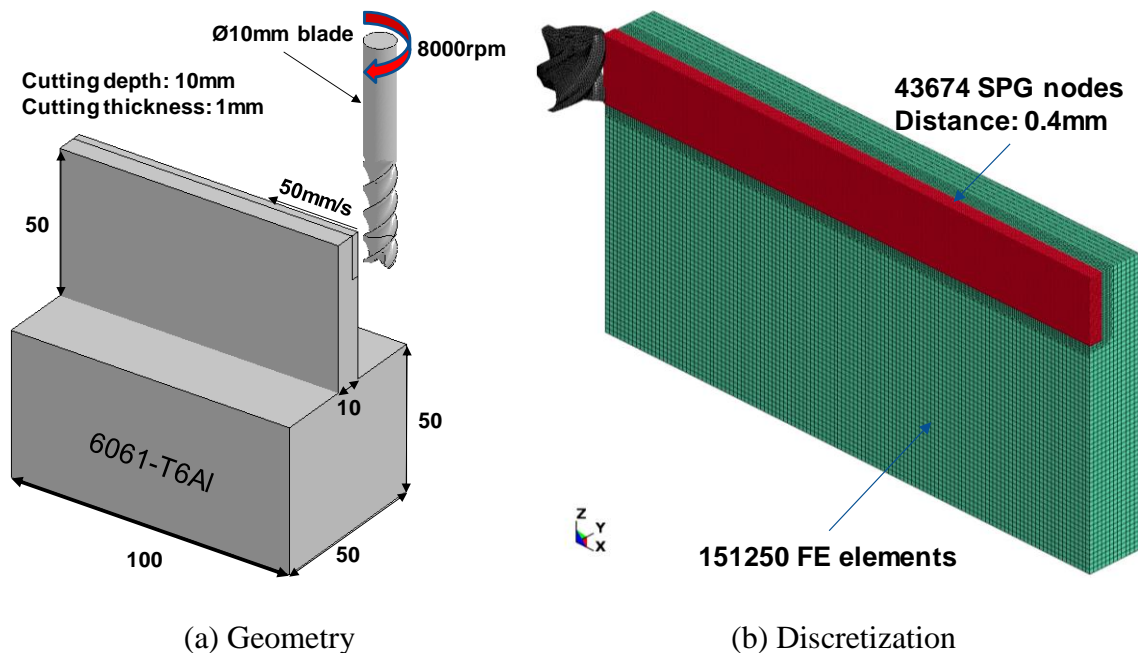(a) Geometry   (b) Discretization

Figure 3. Metal machining: problem statement and discretization.

To obtain reasonable results under a reasonable computational cost, a simplified structure as shown in Figure 3 (b) is used instead, by noticing that the physics will not be changed dramatically by this simplification. In the simplified structure, the cutter is modeled only in its effective length (i.e., in contact with the workpiece) of 10 mm. On the other hand, the workpiece is approximated by its top portion (length 100 mm, height 50 mm and thickness 10 mm) while clamped at the bottom.

To further reduce CPU time, only the vicinity close to the tool is modeled by SPG while the remaining majority of the workpiece is modeled by FEM (Figure 3 (b)). The feasibility of coupling FEM with SPG has been studied earlier[3]. The nodal distance is 0.40 mm in the SPG region and a normalized nodal support size of 1.8 is used for the SPG approximation. Noticing that the deformation in metal machining is quite localized with debris forming, the pseudo-Lagrangian kernel (KERNEL=2) is used for the SPG shape function and is updated every 15 explicit time steps. The standard pin-ball contact algorithm [7] is employed to model the contact

between the tool and workpiece and the coefficient of friction (COF) between the cutter and workpiece is assumed to be 0.5 (www.EngineeringToolBox.con) in the simulation.

4.2. Force responses

Figure 4 shows the comparison of the reaction forces recorded in the test and obtained from various numerical approaches. Figure 4 (a) reveals that the SPG solution matches the test data very well. On the other hand, apparent underestimation is observed for the FEM with erosion solution, which is clearly due to the loss of mass and momentum during element erosion after failure. Figure 5 shows the evolution of the effective plastic strain during the metal machining process (blue: 0.0, red: 0.40). Debris, consisted of by a group of particles, are captured by the SPG approach, which is consistent with the experimental observation. To capture the debris is important in this type of analysis since some sort of protective structure needs to be designed to keep the surrounding equipment from damaging by these debris. Had FEM with erosion been used for the analysis, no debris would be captured since they are all deleted upon failure.
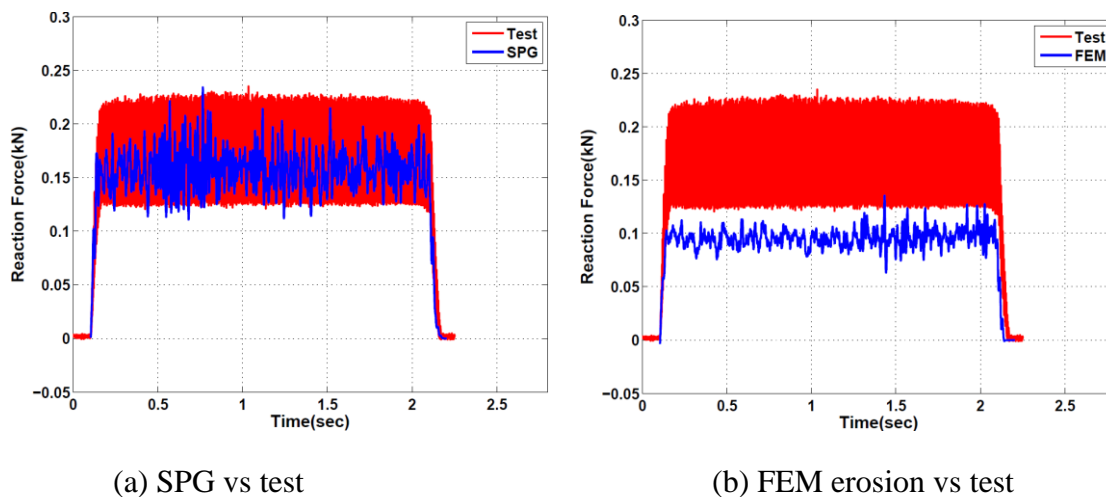

(a) SPG vs test   (b) FEM erosion vs test

Figure 4. Metal machining: force comparisons

@ t = 0.3 sec
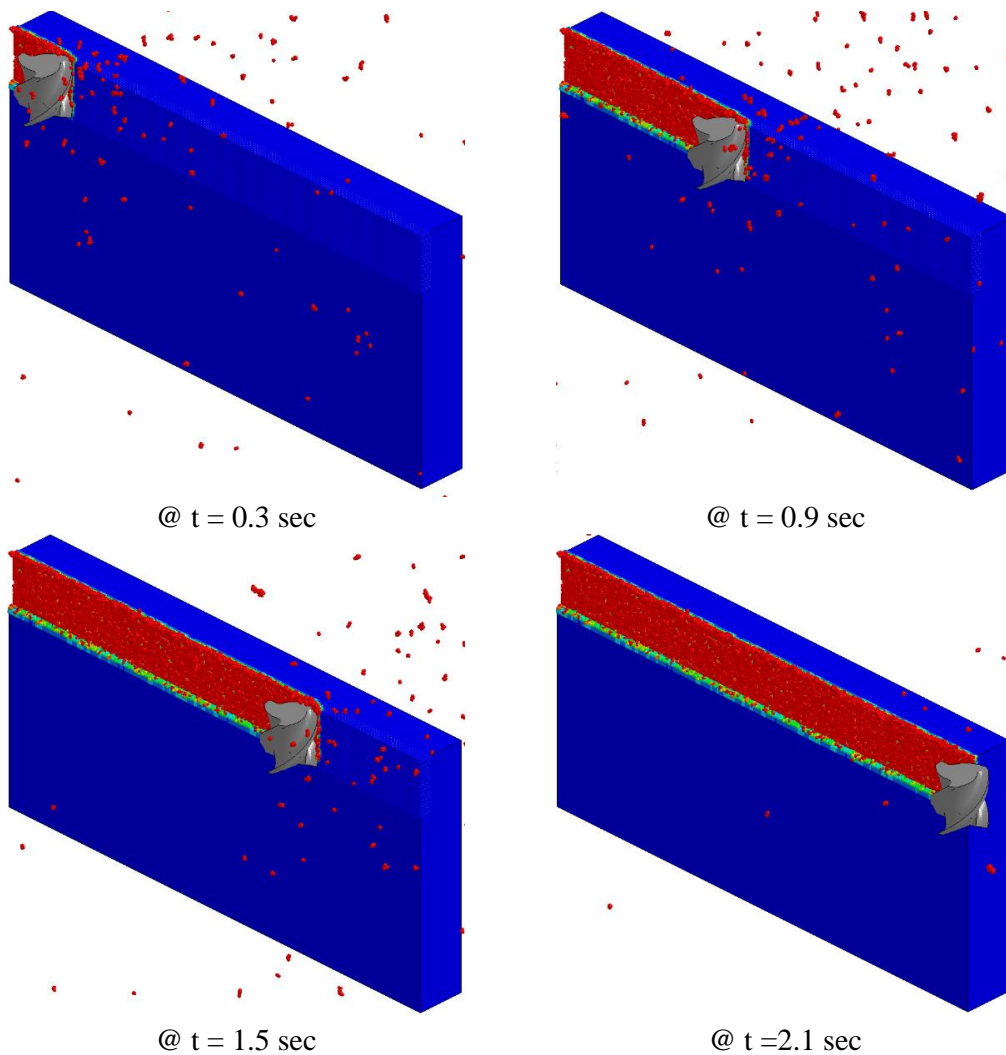
@ t = 0.9 sec

@ t = 1.5 sec

@ t =2.1 sec

Figure 5. Metal machining: evolution of effective plastic strain and debris (SPG).

4.3. SPG parameter sensitivity

Figure 6 shows the parametric study for the metal machining process. Figure 6 (a) demonstrates the convergence behavior of the SPG formulation numerically. The numbers on the legend indicate the nodal distances in the SPG discretizations. Since the cutting thickness is 1.0 mm, nodal distance of 0.30 mm indicates 4 nodes will be removed during the machining process, 0.40 mm results in 3 nodes removal in the process, and 0.75 mm nodal distance results in 2 nodes removal. Clearly, the numerical solution converges as the discretization is refined.

Figure 6 (b) plots the reactions forces obtained with various bond failure criteria. The force does not seem to be very sensitive to the SPG bond failure criteria: critical effective plastic strain of 0.2 (FS0.2) or 0.4 (FS0.4). However, higher oscillation is observed for the case of FS0.4, which is possibly due to a little excessive straining, which in turn implies that the failure criteria might have been set improperly (a little too high for physical failure to occur). Figure 6 (c) plots the reaction forces obtained with various kernel update frequencies: 30 (SM30), 15 (SM15) and 5 (SM05) explicit time steps respectively. Very marginal sensitivity to the kernel update interval is observed. Figure 6 (d) shows the reaction forces obtained with various normalized support

size: 1.6 (SP1.6) and 1.8 (SP1.8). The numerical results do not show strong dependence on the normalized support size.
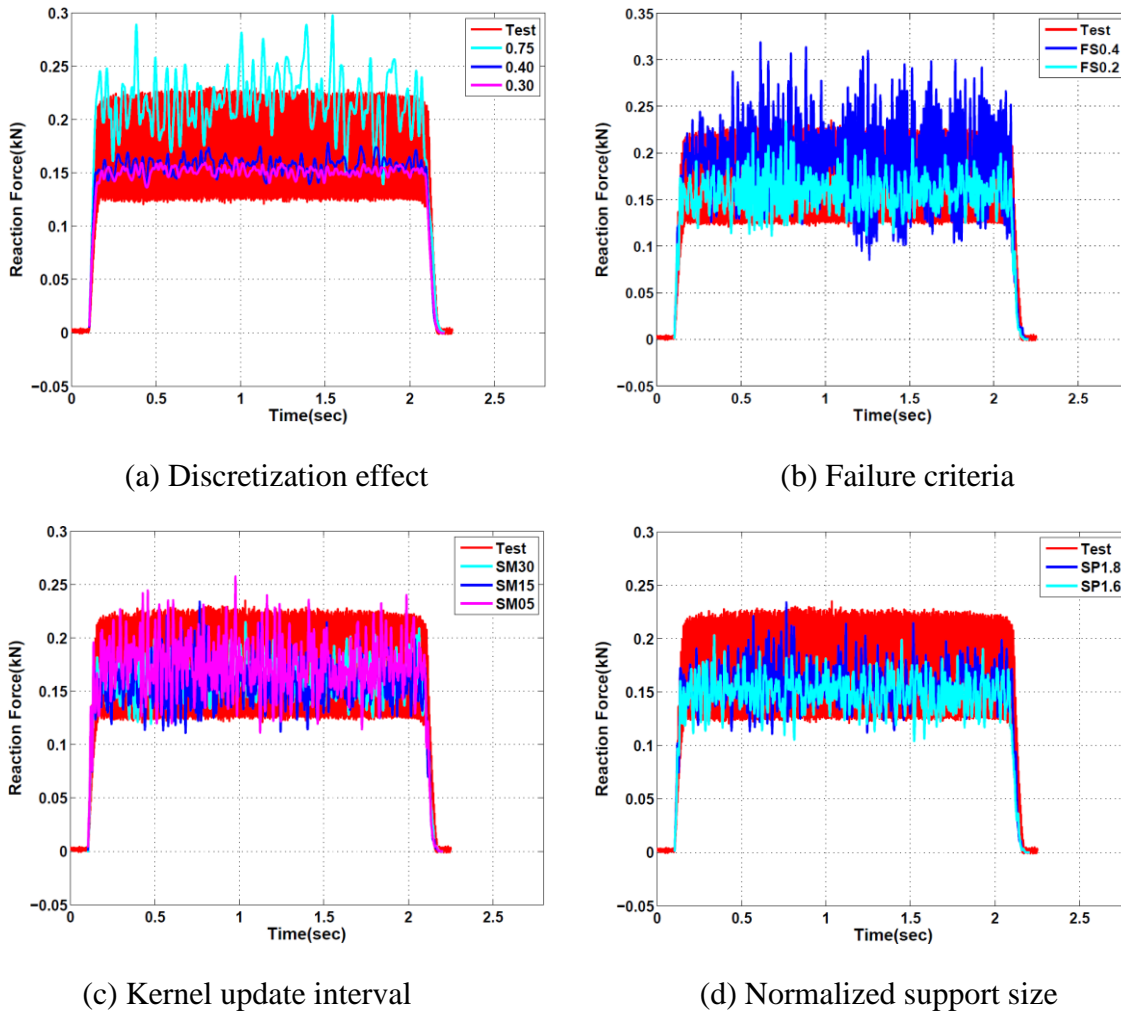

(a) Discretization effect

(b) Failure criteria

(c) Kernel update interval

(d) Normalized support size

Figure 6. Metal machining: SPG parameter sensitivity.

5. SPG for semi-brittle failure analysis

The effectiveness of the SPG method in modeling semi-brittle failure is demonstrated in this section through the analysis of a projectile impacting on a concrete slab. Convergence and parametric studies are also carried out.

5.1. Geometry and discretization

The test was reported by Hanchak et al [8]. A square reinforced concrete slab with dimension of 610x610x178 mm was used in the test, which is schematically shown in Figure 7 (a). The slab is simply supported at two opposite edges. The unconfined compressive strength of the concrete is 48 MPa. The slab was hit at the center perpendicularly by a diameter of 25.4 mm and length 144 mm ogival-nose projectile at a velocity of 750 m/s. The mass of the projectile is 0.53 kg.

The rebar is not modeled in this study since the reinforcement does not have a significant impact on the residual velocity of the projectile [8]. As shown in Figure 7 (b), the projectile is modeled as elastic. To reduce computational cost, only a small portion of the concrete slab is approximated by the SPG formulation and the majority is modeled by FEM. The nodal distance in the SPG region is approximately 4.1 mm in-plane and 6.4 mm out-of-plane and a normalized support size of 1.4 is used for the SPG approximation. The K&C concrete constitutive model (mat072r3) is used to model the behavior of the concrete and accordingly, the FS for SPG bond failure is set to 1.98, which corresponds to a strength reduction of about 95% before failure and the stretch for concrete is usually no more than 1% (STRETCH=1.01). The damage in a projectile impact is usually very localized, therefore, the pseudo-Lagrangian kernel (KERNEL=2) is used for the SPG approximation and is updated every 30 explicit time steps. The interaction between the failed particles on the path of perforation is captured by the SPG self-contact algorithm (set ISC to the Young's modulus of the concrete). The standard pin-ball contact algorithm is used to model the contact between the projectile and concrete slab. A static COF of 0.05 is assumed in the simulation.
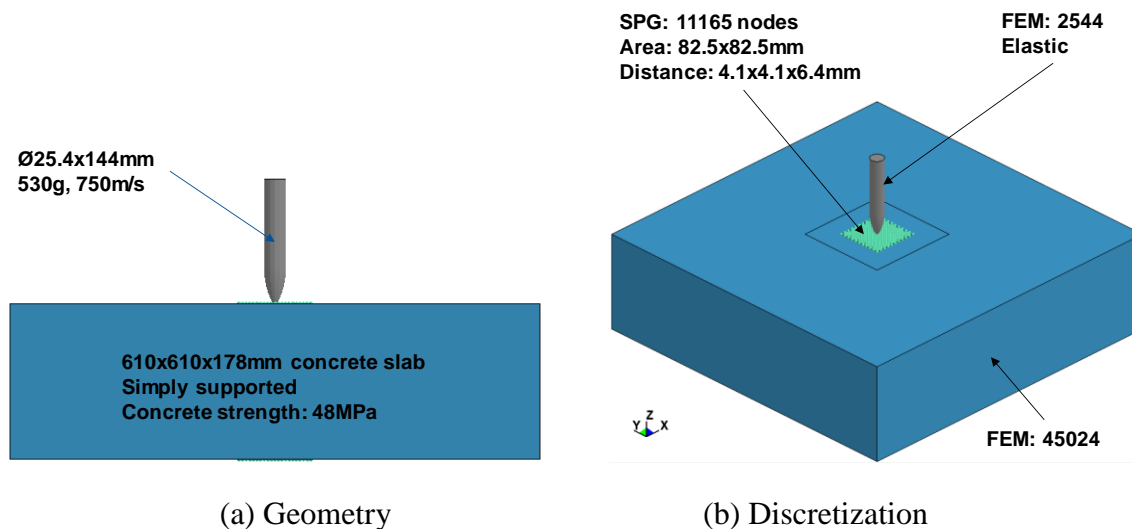

| (a) Geometry | (b) Discretization |

Figure 7. Perforation of concrete slab: problem statement and discretization.

5.2.   General responses

Figure 8 shows the projectile velocity history against time and depth of penetration (DOF). DOF here is actually the displacement of the projectile in the impact (z-) direction. The projectile approaches a constant velocity after certain time / DOF, which indicates a perforation response. It is also seen that the projectile reaches its residual velocity, which is comparable with the experimental value, after a DOF of barely about the thickness of the slab, which is physical since concrete is a semi-brittle material. Furthermore, an approximately constant deceleration is obtained which is typical in impact penetration and perforation responses. Figure 9 shows the concrete material damage after perforation. The damage is very localized, which is consistent with the physics in this type of test. Material loses all strength when damage reaches 2.0 if no confinement is applied.
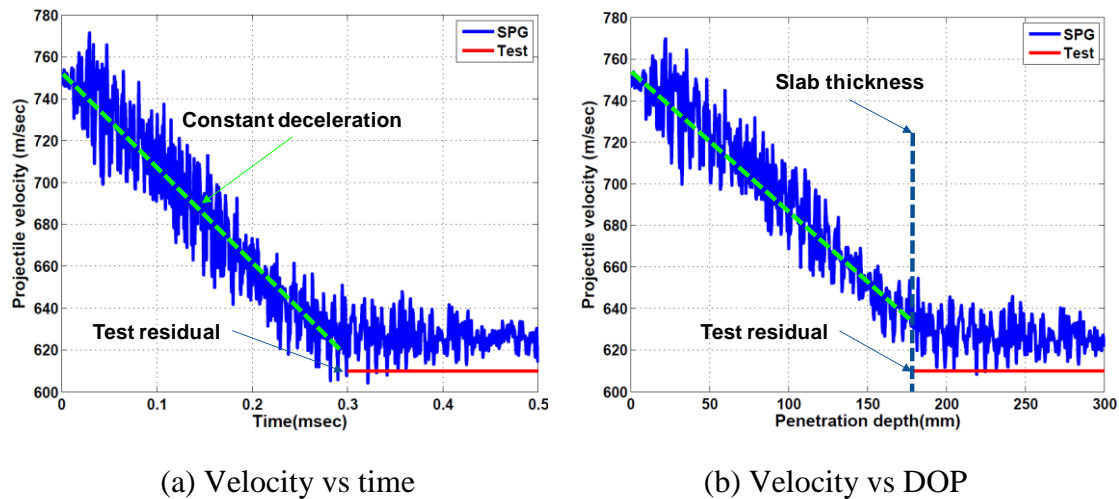
(a) Velocity vs time   (b) Velocity vs DOP

Figure 8. Perforation of concrete slab: velocity history.

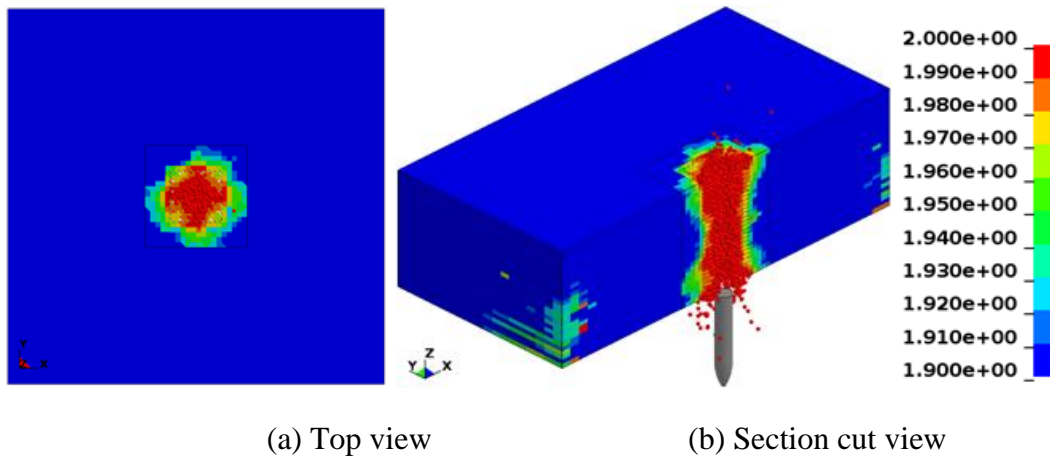(a) Top view   (b) Section cut view

Figure 9. Perforation of concrete slab: damage at termination.

5.3. SPG parametric study

Figure 10 (a) compares the numerical results obtained from three discretizations with the experimental data. The legend refers to the nodal distance in SPG discretization in x-, y-, and z-directions respectively. All the numerical results are close to each other, which indicates that the solution is nearly mesh independent. It can also be concluded that the SPG solution converges from this observation.

Figure 10 (b) shows the results obtained using different SPG bond failure criteria. "FS0.95" indicates that SPG bond failure occurs at 95% strength reduction and "FS0.30" refers to bond failure at 30% strength reduction. With such a huge difference on the failure criteria, the numerical responses are still quite close to each other, which is drastically different from FEM with erosion approach. This insensitivity to bond failure criteria might be because the problem is momentum driven, which mitigates the solution dependence on material strength.

Figure 10 (c) compares the SPG solutions obtained with various kernel update intervals with the test residual, and Figure 10 (d) examines the SPG solutions with various normalized support sizes. The dependence on these parameters is insignificant.
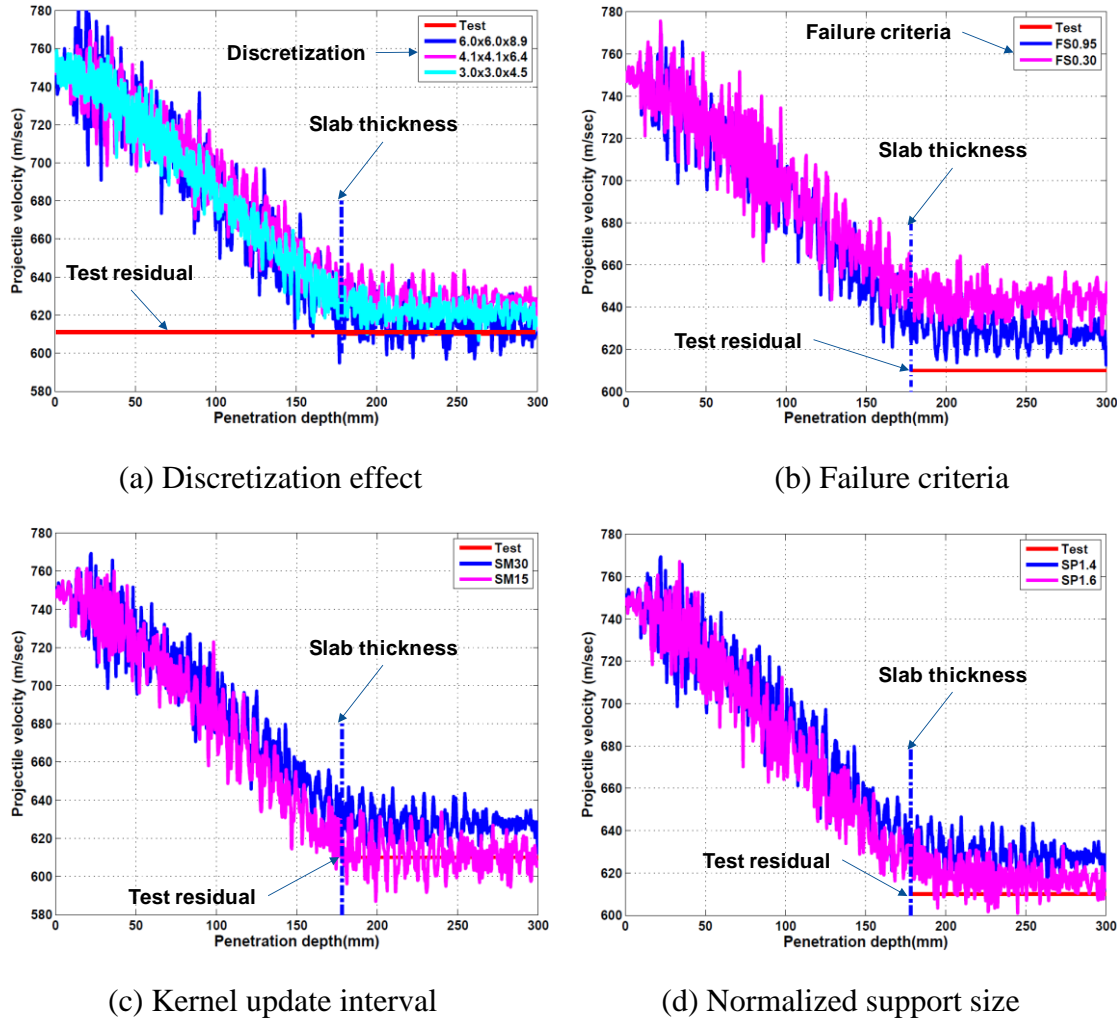

(a) Discretization effect

(b) Failure criteria

(c) Kernel update interval

(d) Normalized support size

Figure 10. Perforation of concrete slab: SPG parameter sensitivity.

6. Conclusion

In this paper, the smoothed particle Galerkin (SPG) method is applied in the analysis of ductile and semi-brittle material failure processes. To deal with material failure in large deformation manufacturing and impact penetration processes, a bond-based failure mechanism is implemented under the SPG framework. With the bond failure mechanism, mass and momentum are conserved during material failure modeling, which is very important in correctly predicting reaction forces and failure modes and is in sharp comparison with element erosion type of failure mechanism in finite element models.

Metal machining (ductile) and perforation concrete slab (semi-brittle) are analyzed with the SPG method. Very promising results are obtained both qualitatively and quantitatively. Convergent and stable responses are

obtained. Parametric studies showed that the numerical results are negligibly sensitive to the SPG bond failure criteria for both ductile and semi-brittle materials, which makes the numerical scheme robust and reliable since the bond failure criteria do not need to be tuned, which once again compares dramatically different from element erosion type finite element analysis. However, it should still be emphasized that to obtain physical response, the parameters should be as physical as possible. Parametric studies also revealed that the numerical results are marginally sensitive to the SPG parameters such as the normalized support size and the kernel update interval.

Reference

[1]   Wu CT, Koishi M, Hu W. A displacement smoothing induced strain gradient stabilization for the meshfree Galerkin nodal integration method. *Comput. Mech.* **56**, 19-37, 2015.

[2]   Wu CT, Chi SW, Koishi M, Wu Y. Strain gradient stabilization with dual stress points for the meshfree nodal integration method in inelastic analysis. *Int. J. Numer. Methods Engrg.* **107**, 3-30, 2016.

[3]   Wu CT, Bui TQ, Wu Y, Luo TL, Wang M, Liao CC, Chen PY, Lai YS. Numerical and experimental validation of a particle Galerkin method for metal grinding simulation. *Comput. Mech*. https://doi.org/10.1007/s00466-017-1456-6, 2017.

[4]   Wu CT, Wu Y, Crawford JE, Magallanes JM. Three-dimensional concrete impact and penetration simulations using the smoothed particle Galerkin method. *Int. J. Impact Engrg.* **106**, 1-17, 2017.

[5]   Wu Y, Wu CT. Simulation of impact penetration and perforation of metal targets using the smoothed particle Galerkin method. Accepted, *J. Engrg. Mech.* 2017.

[6]   Wu CT, Wu Y, Koishi M. A Strain-morphed Nonlocal Meshfree Method for the Regularized Particle Simulation of Elastic-damage Induced Strain Localization Problems. *Comput. Mech.* **56 (6)**, 1039-1054, 2015.

[7]   Belytschko T, Liu WK, Moran B, Elkhodary KI. Nonlinear Finite Elements for Continua and Structures, Second Edition, John Wiley & Sons, Ltd., United Kingdom, 2014

[8]   Hanchak SJ, Forrestal MJ, Young ER, Erhrgoott JQ. Perforation of concrete slabs with 48 MPa (7 ksi) and 140 MPa (20ksi) unconfined compressive strengths. *Int. J. Impact Engrg.,* **12**, 1-7, 1992